

# Dual lead-crowning for helical gears with anti-twist tooth flanks on the internal gear honing machine

Van-Quyet Tran and Yu-Ren Wu\*

Department of Mechanical Engineering, National Central University, 300, Jhongda Rd., Jungli City, Taoyuan 320, Taiwan, R.O.C.

\*E-mail: yurenwu@ncu.edu.tw

**Abstract.** For some specific purposes, a helical gear with wide face-width is applied for meshing with two other gears simultaneously, such as the idle pinions in the vehicle differential. However, due to the fact of gear deformation, the tooth edge contact and stress concentration might occur. Single lead-crowning is no more suitable for such a case to get the appropriate position of contact pattern and improve the load distribution on tooth surfaces. Therefore, a novel \*Email: method is proposed in this paper to achieve the wide-face-width helical gears with the dual lead-crowned and the anti-twisted tooth surfaces by controlling the swivel angle and the rotation angle of the honing wheel respectively on an internal gear honing machine. Numerical examples are practiced to illustrate and verified the merits of the proposed method.

## 1. Introduction

In some specific applications, the helical gears with wide face-width are applied for meshing with another two gears simultaneously, such as those idle pinions in the helical gear-type vehicle limited slip differential (EATON Detroit Truetrac®). For such a case, one half of the tooth flank of a pinion meshes with one side gear and another half meshes with one other pinion for distributing the transmission power. However, the gear tooth deformation and deflection might occur due to the large torque, leading to the possibilities of appearance of the tooth edge contact and early gear damage. Based on evidence that the helical gears with crowned and twist-free tooth flanks can enhance the load capacity, reduce the risk for high concentrated contact pressure and extend life-span, how to achieve the tooth modification on two half tooth flanks for this case is really worthy to study further.

In the past, several studies about the gear honing have been presented. Dugas [1] and [2] presented the research about rotary gear honing such as working process of honing machine and honing tool. Wright and Schriefer [3] presented some discussions about the gear honing process as well as advantages of internal gear honing. Klocke [4] introduced axes motions and combinations on the internal gear honing machine for removing material of tooth flank on the work gear surface. Mehta and Rath [5] mentioned about the internal gear honing is the most efficient process of gear finishing. Besides, Amini et al. [6] conducted an experimental study of gear abrasive wear for reducing noise. Moreover, some published studies mentioned about single lead-crowning for helical gear. Tran et al. [7]–[8] proposed a crowning method by controlling an additional rotation angle of the work gear during the hobbing process. Further, Wu and Tran [9]–[10] proposed a method by controlling the



crossed angle between axes of the honing cutter and the work gear to achieve the crowned and twist-free helical tooth flanks using a variable pressure angle (VPA) honing wheel.

Referring to the aforementioned studies and the encountered problem, a novel method to obtain a helical gear with dual lead-crowned tooth flanks using the internal gear honing process is proposed in this paper. Two additional motions are given for achieving the dual lead-crowning and the twist-free tooth surfaces by setting the swivel angle of honing wheel a linear function of axial feed of honing wheel and by adding the rotation angle of work gear a product of the rotation angle of honing wheel and the axial feed of honing wheel with a coefficient, respectively. Based on the proposed method, two numerical examples are carried out to prove the practicability and validity of this method.

## 2. Mathematical model of generation of standard honing wheel

As shown in figure 1, the position vector and the unit normal vector on right surface of the rack can be expressed in the coordinate system  $S_r(x_r, y_r, z_r)$  as follows:

$$\mathbf{r}_r(u, v) = [x_r, y_r, z_r, 1]^T = [u \cos \alpha_{pa}, w - u \sin \alpha_{pa}, v, 1]^T \quad (1)$$

$$\mathbf{n}_r(u, v) = [x_{nr}, y_{nr}, z_{nr}]^T = [\sin \alpha_{pa}, -\cos \alpha_{pa}, 0]^T \quad (2)$$

where  $u$  and  $v$  are the surface parameters of rack,  $\alpha_{pa}$  is the pitch pressure angle of standard rack and  $w$  is a quarter of tooth pitch and can be calculated by  $w = \pi m_n / 4$ , wherein  $m_n$  is the normal module.

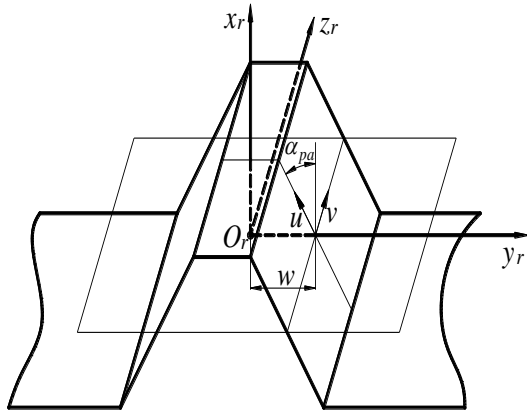


**Figure 1.** Geometric schematics of the rack.

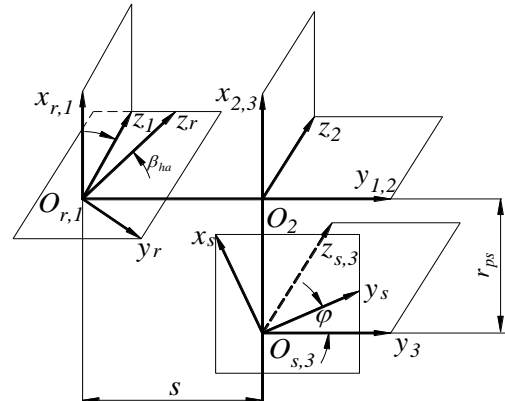


**Figure 2.** Relative motion coordinate systems between rack and helical gear.

As shown in figure 2, the helical gear can be generated by rack according to the relative motion relationship. Where the coordinate systems  $S_r(x_r, y_r, z_r)$ ,  $S_s(x_s, y_s, z_s)$  and  $S_3(x_3, y_3, z_3)$  are rigidly attached to the rack, helical gear and frame, respectively. Then, the equations of locus and unit normal vector of rack in  $S_s$  can be obtained by transforming from  $S_r$  to  $S_s$  as follows:

$$\mathbf{r}_s(u, v, \varphi) = \mathbf{M}_{sr}(\varphi) \cdot \mathbf{r}_r(u, v) \quad (3)$$

$$\mathbf{n}_s(u, v, \varphi) = \mathbf{L}_{sr}(\varphi) \cdot \mathbf{n}_r(u, v) \quad (4)$$

where  $\mathbf{M}_{sr}(\varphi)$  is the transformation matrix from  $S_r$  to  $S_s$ ,  $\mathbf{L}_{sr}(\varphi)$  is the upper-left  $3 \times 3$  submatrix of  $\mathbf{M}_{sr}(\varphi)$ . Symbols  $\varphi$  and  $r_{ps}$  are the rotation angle and operating pitch radius of the generated helical gear, respectively. And  $s$  is the displacement of rack, it can be calculated by  $s = r_{ps} \varphi$ .

According to the theory of gearing (Litvin [11]), the meshing condition between the right rack surface and the right helical gear surface can be established by:

$$f_1(u, v, \varphi) = \mathbf{n}_s \cdot \frac{\partial \mathbf{r}_s(u, v, \varphi)}{\partial \varphi} = 0 \quad (5)$$

As shown in figure 3, the honing wheel can be generated by the helical gear using the homogenous coordinate transformation from  $S_s$  to  $S_h$  (the moving coordinate system of honing wheel). The equations of locus and unit normal vector of rack can be represented in  $S_h$  as follows:

$$\mathbf{r}_h(u, v, \varphi, \theta_h) = \mathbf{M}_{hs}(\theta_h) \cdot \mathbf{r}_s(u, v, \varphi) \quad (6)$$

$$\mathbf{n}_h(u, v, \varphi, \theta_h) = \mathbf{L}_{hs}(\theta_h) \cdot \mathbf{n}_s(u, v, \varphi) \quad (7)$$

where  $\mathbf{M}_{hs}(\theta_h)$  is the transformation matrix from  $S_s$  to  $S_h$ ,  $\mathbf{L}_{hs}(\theta_h)$  is the upper-left  $3 \times 3$  submatrix of  $\mathbf{M}_{hs}(\theta_h)$ . Symbols  $\theta_s$  and  $\theta_h$  are the rotation angle of helical gear and honing wheel, respectively. Besides,  $\theta_h$  can be calculated by  $\theta_h = N_s \varphi / N_h$ , wherein  $N_s$  and  $N_h$  are the tooth number of helical gear and honing wheel, respectively. And  $r_{ps}$  and  $r_{ph}$  are operating pitch radii of generated helical gear and honing wheel, respectively. The symbol  $E_o$  is the centre distance between helical gear and honing wheel.

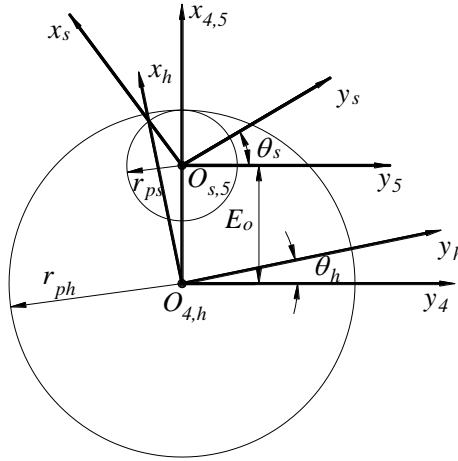


**Figure 3.** Relative motion coordinate systems between helical gear and honing wheel.

The meshing condition between the right helical gear surface and right honing wheel surface can be obtained by:

$$f_2(u, v, \varphi, \theta_h) = \mathbf{n}_h \cdot \frac{\partial \mathbf{r}_h(u, v, \varphi, \theta_h)}{\partial \theta_h} = 0 \quad (8)$$

Finally, the equation of honing wheel surface can be obtained by solving Eq.s (5), (6) and (8) simultaneously.

### 3. Dual lead-crowning of helical gear on internal gear honing machine

#### 3.1 Mathematical model

As shown in figure 4, the 3-D schematic of an internal gear honing machine (Fässler HMX-400) shows eight moving axes for gear honing, wherein  $T_1$ ,  $T_2$  and  $T_3$  are three translational motion axes in the radial, tangential and axial feed axes respectively,  $R_1$  is the swivel axis of honing-stone head for lead crowning,  $R_2$  is the swivel axis of the honing stone for adjusting the axis-crossing angle,  $R_3$  is the swivel axis of headstock turntable,  $R_4$  is the spindle axis of workpiece and  $R_5$  is the spindle axis of honing wheel. This machine is then used in this paper to practice the dual lead-crowning on helical gears.

The relative motion coordinate systems between the honing wheel and the workpiece are established in figure 5, the coordinate systems  $S_c(x_c, y_c, z_c)$  and  $S_w(x_w, y_w, z_w)$  are rigidly attached to the honing wheel and work gear, respectively, the coordinate system  $S_s(x_s, y_s, z_s)$  is rigidly attached to the

frame of honing machine, while  $S_6(x_6, y_6, z_6)$ ,  $S_7(x_7, y_7, z_7)$ ,  $S_9(x_9, y_9, z_9)$  and  $S_d(x_d, y_d, z_d)$  are auxiliary coordinate systems for the simplification of coordinate transformation.

For lead-crowning of a work gear, a linear function of axial motion of the work gear is given to the swivel angle of honing wheel around the  $R_2$  axis,  $\phi_w$ , as the following equation:

$$\phi_w = kt \quad (9)$$

where  $k$  is an adjusting coefficient of the swivel angle, and  $t$  is honing wheel's feed along  $T_2$  axis.

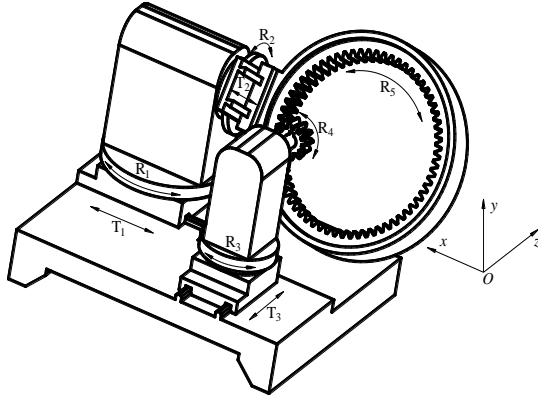


**Figure 4.** 3-D schematic of a CNC internal gear honing machine.

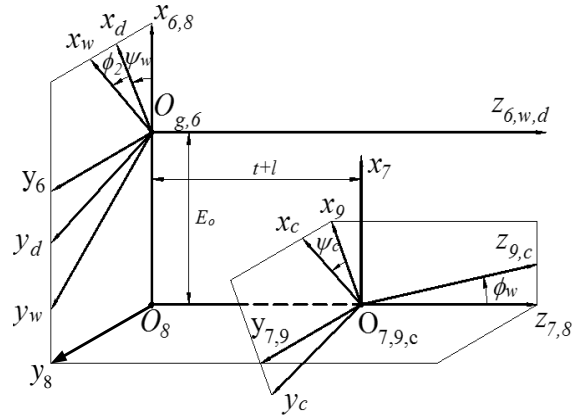


**Figure 5.** Coordinate systems for F äsler HMX-400 internal gear honing machine.

By applying the homogeneous coordinate transformation from  $S_c$  to  $S_w$ , the equations of locus and unit normal vector of the honing wheel can be represented in the coordinate system  $S_w$  as follows:

$$\mathbf{r}_w(u, v, \varphi, \theta_h, \psi_c, t) = \mathbf{M}_{wc}(\psi_c, t) \cdot \mathbf{r}_h(u, v, \varphi, \theta_h) \quad (10)$$

$$\mathbf{n}_w(u, v, \varphi, \theta_h, \psi_c, t) = \mathbf{L}_{wc}(\psi_c, t) \cdot \mathbf{n}_h(u, v, \varphi, \theta_h) \quad (11)$$

where  $\mathbf{M}_{wc}$  is the transformation matrix from  $S_c$  to  $S_w$ , and  $\mathbf{L}_{wc}$  is the upper-left  $3 \times 3$  submatrix of  $\mathbf{M}_{wc}$ . All elements in  $\mathbf{M}_{wc}$  are listed as follows:

$$\mathbf{M}_{wc} = \begin{bmatrix} a_{11} & a_{12} & a_{13} & a_{14} \\ a_{21} & a_{22} & a_{23} & a_{24} \\ a_{31} & a_{32} & a_{33} & a_{34} \\ 0 & 0 & 0 & 1 \end{bmatrix} \quad (12)$$

wherein,  $a_{11} = \cos \phi_w \cos \psi_c \cos(\phi_2 - \psi_w) + \sin \psi_c \sin(\phi_2 - \psi_w)$ ,

$a_{12} = \cos \psi_c \sin(\phi_2 - \psi_w) + \cos \phi_w \cos(\phi_2 - \psi_w)$ ,  $a_{13} = \sin \phi_w \cos(\phi_2 - \psi_w)$ ,  $a_{14} = -E_o \cos(\phi_2 - \psi_w)$ ,

$a_{21} = \cos \phi_w \cos \psi_c \sin(\phi_2 - \psi_w) + \sin \psi_c \cos(\phi_2 - \psi_w)$ ,  $a_{22} = \cos \psi_c \cos(\phi_2 - \psi_w) - \sin \phi_w \sin(\phi_2 - \psi_w)$ ,

$a_{23} = \sin \phi_w \sin(\phi_2 - \psi_w)$ ,  $a_{24} = -E_o \sin(\phi_2 - \psi_w)$ ,  $a_{31} = -\sin \phi_w \cos \psi_c$ ,  $a_{32} = \sin \phi_w \sin \psi_c$ ,  $a_{33} = \cos \phi_w$  and

$a_{34} = t + \ell$ .

In the above equations, the symbols  $\psi_w$  and  $\psi_c$  are the rotation angles of the work gear and the honing wheel, respectively, and  $\phi_2$  is the rotation angle of work gear and  $\ell$  is the distance between two central cross-sections where the dual lead-crowning starts (see in figure 6).

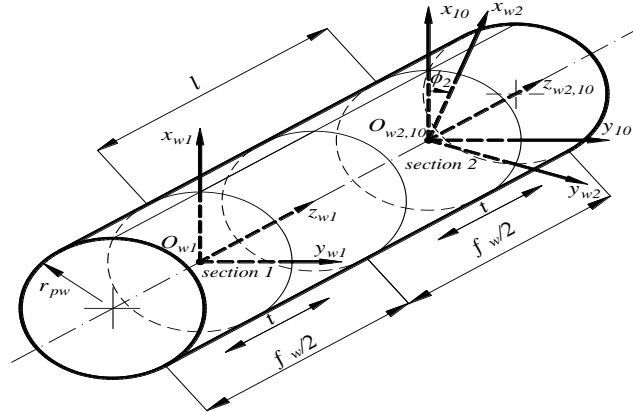


**Figure 6.** Dual lead-crowning on wide-face-width work gear during honing process.

As shown in figure 6, the dual lead-crowning process can be performed through the following strategy: the tooth flank of work gear is considered to be divided into two parts with the same length. For honing the first half of tooth flank, the honing wheel moves along the axis of work gear and meshes with the work gear at the position of section 1, where  $\phi_2 = 0$  and  $a_{34} = t$  ( $\ell = 0$ ) are given; and then for the another half of tooth flank, the honing wheel moves axially and meshes with work gear at the position of section 2, where  $\phi_2 = f_w / (2r_{pw} \cos \beta_{ha})$  and  $a_{34} = t + f_w / 2$  ( $\ell = f_w / 2$ ) are defined, wherein  $f_w$  is the face width of tooth gear,  $r_{pw}$  is the operating pitch radius of work gear and  $\beta_{ha}$  is the helical angle of honing wheel.

The meshing conditions between the right honing surface and right work gear surface can be obtained by the following two equations:

$$f_3(u, v, \varphi, \theta_h, \psi_c, t) = \mathbf{n}_w \cdot \frac{\partial \mathbf{r}_w(u, v, \varphi, \theta_h, \psi_c, t)}{\partial \psi_c} = 0 \quad (13)$$

$$f_4(u, v, \varphi, \theta_h, \psi_c, t) = \mathbf{n}_w \cdot \frac{\partial \mathbf{r}_g(u, v, \varphi, \theta_h, \psi_c, t)}{\partial t} = 0 \quad (14)$$

The rotation angle of work gear,  $\psi_w(\psi_c, t)$  can be calculated according to the following equation:

$$\psi_w = \frac{N_c}{N_w} \psi_c + \tan \beta_{ha} \left( \frac{kr_{ph} - 1}{r_{pw}} \right) t + b\psi_c t \quad (15)$$

where  $N_c$  and  $N_w$  denote tooth numbers of the honing wheel and the work gear respectively,  $\psi_c$  and  $\psi_w$  are the rotation angles of honing wheel and work gear respectively, and  $b$  is the correction coefficient for generating the twist-free tooth surface.

### 3.2 Normal deviation of the work gear tooth surface

The normal deviation of work gear tooth flank can be obtained by comparing the machined gear tooth flank with the standard gear tooth flank. The normal deviations at each grid points can be computed by the following equation:

$$\delta_{ij} = (\mathbf{r}_{w,ij} - \mathbf{r}_{s,ij}) \cdot \mathbf{n}_{s,ij}, \quad i = 1 \sim 13, j = 1 \sim 13 \quad (16)$$

To obtain dual lead-crowned and anti-twist tooth flanks for the work gear, a flowchart for determining coefficients  $k$  and  $b$  is given as figure 7 shows.

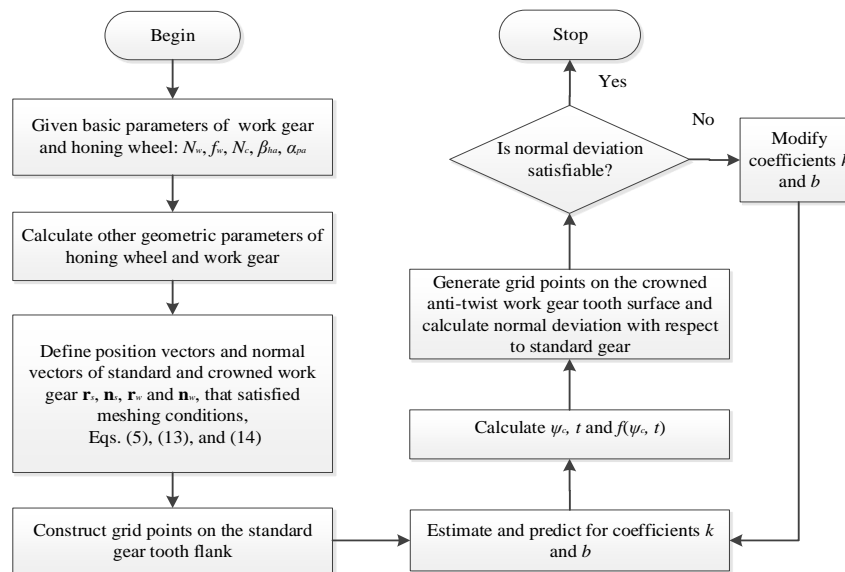


**Figure 7.** Flowchart for determination of coefficients  $k$  and  $b$ .

## 4. Numerical examples

### 4.1. Dual lead-crowning for a helical gear with anti-twisted tooth surfaces by gear honing process

To demonstrate the proposed method, two cases with different coefficients  $b=0$  (Case A) and coefficient  $b = -2.75 \times 10^{-3}$  (Case B) and the same coefficient  $k = -3.50 \times 10^{-3}$  are carried out to show two different dual lead-crowned gear tooth surfaces, which are with and without anti-twisted tooth flank corrections, in forms of tooth surface topographies. The related parameters for this example are given in table 1.

**Table 1.** Related parameters of work gear and honing wheel.

Work gear	Value [Unit]
Number of teeth ( $N_g$ )	12
Normal module ( $m_n$ )	2.0 [mm]
Normal pressure angle ( $\alpha_{pa}$ )	30.0 [degree]
Pitch helix angle ( $\beta_{ha}$ )	20.0 [degree]
Face width ( $f_w$ )	40.0 [mm]
Honing wheel	
Number of teeth ( $N_h$ )	120
Normal module ( $m_n$ )	2.0 [mm]

Moreover, two indices are proposed for evaluating the twist degree of machined gear tooth surfaces, wherein one is the maximum tooth flank twist,  $M_{tf}$ , which is defined by the largest crowning amount subtract the smallest crowning amount; and another one is the crowning evenness ratio,  $C_{er}$ , which is defined by the smallest crowning amount divided by the largest crowning amount. For an anti-twisted tooth surface,  $M_{tf}$  is as smaller as better and  $C_{er}$  is as larger as better.

To validate the proposed dual lead-crowning method, the topographies of work gear tooth surfaces without applying an anti-twist tooth surface correction (Case A) and with applying an anti-twist tooth surface correction (Case B) are practiced. As the comparison shown in figure 8, the index  $M_{tf}$  for the first part (upper parts) lead-crowned tooth surface is reduced from 16.08  $\mu\text{m}$  (Case A) to 4.59  $\mu\text{m}$  (Case B) and  $C_{er}$  is improved from 0.23 (Case A) to 0.71 (Case B). Besides, for the second part (lower parts) tooth surface,  $M_{tf}$  is reduced from 15.86  $\mu\text{m}$  (Case A) to 6.39  $\mu\text{m}$  (Case B) and  $C_{er}$  is improved from 0.21 (Case A) to 0.59 (Case B). From the results of these two cases, the proposed method is proved that the anti-twisted gear tooth surface can be attained in the dual lead-crowning process.



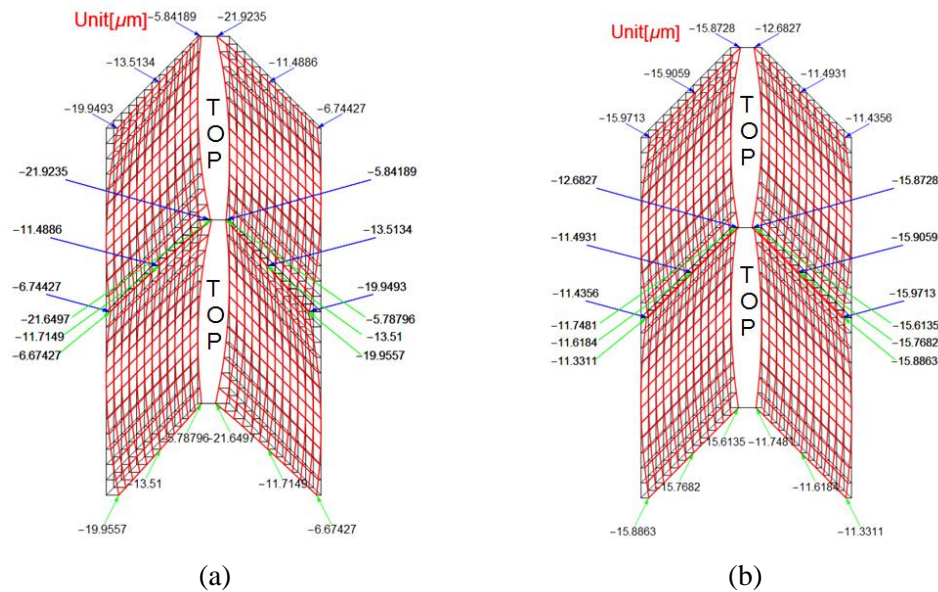


**Figure 8.** Topographies of dual lead-crowned gear surfaces: (a) Case A ( $b = 0$ ) and (b) Case B ( $b = -2.75 \times 10^{-3}$ ).

#### 4.2. Tooth contact analysis on the dual lead-crowned tooth surface

As shown in figure 9(a), a possible application for the dual lead-crowned gears is considered in this example, where Gear 1 is the driving gear meshing with another two gears, Gear 2 and Gear 3, simultaneously. The related parameters for these three gears can be seen in table 2.

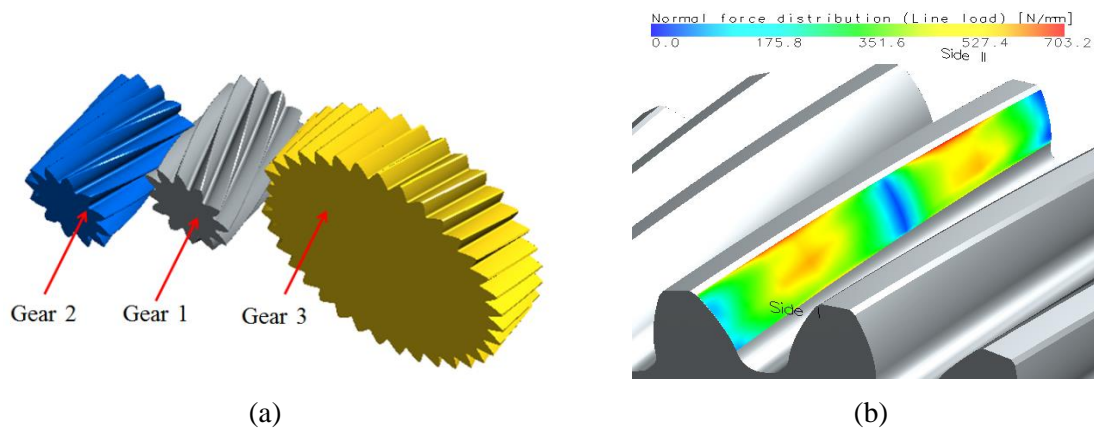


**Figure 9.** Three-gear train and its TCA result: (a) 3-D model, (b) Normal force distribution.

The tooth contact analysis (TCA) of this gear train is conducted with the input power of 60 kW and the input rotation speed of 1000 rpm to display the effect of applying dual lead-crowning on the Gear 1 by giving  $k = -3.5 \times 10^{-3}$  and  $b = -2.75 \times 10^{-3}$ . As the TCA result show in figure 9(b), the tooth contact pattern is obviously divided into two elliptical zones at the centers of two half tooth flank sections and no edge contact occurs on both end sides of tooth flank. Although the higher contact forces appear at the tooth tips of two half sections, but these situations occur generally on the tooth surface with or without lead crowning while the profile modification of tooth tip or root is not applied. by this example, it displays the merit of the proposed dual lead-crowning method because of no normal force concentrations on both end edges of Gear 1 tooth flank under loads, as well as on Gear 2 and Gear 3.

**Table 2.** Parameters for three gears.

Parameters	Gear 1	Gear 2	Gear 3
Number of teeth	12	12	36
Tooth Face-width	40.0 [mm]	40.0 [mm]	20.0 [mm]
Normal module		2.0 [mm]	
Normal pressure angle		30.0 [degree]	
Helical angle		20.0 [degree]	

## 5. Conclusion

A dual lead-crowning method for wide face-width gears using the internal honing machine is proposed in this paper. The mathematical models of honing wheel generation and gear honing process are also established. By controlling swivel angle of the honing stone and giving an additional rotation angle function for work gear, the dual lead-crowned and anti-twist gear tooth flanks can be achieved. Additionally, the numerical examples display the merits of the proposed method by means of topographies of generated gear tooth surfaces and TCA in a possible application for this kind of gear with dual lead-crowned tooth surfaces.

## Acknowledgments

The authors are grateful to the Ministry of Science and Technology of Taiwan (R.O.C.) for the financial support under the projects No: MOST 105-2221-E-008-047.

## References

- [1] J P Dugas 1988 *Rotary Gear Honing, The 16th Annual AGMA Gear Symposium* pp 36–38
- [2] J P Dugas 1992 *Gear Finishing by Shaving, Rolling & Honing - Part II, Gear Technology* pp 24–30
- [3] N W Wright and H Schriefer 1997 “Basic Honing and Advanced Free-Form Honing,” *Gear Technology, Vol. 204* pp 26–33
- [4] F Klocke 2009 “Manufacturing Processes 2-Grinding, Honing, Lapping,” *RWTHedition, RWTH Aachen* pp 334–337
- [5] D T Mehta and M G Rath 2013 “A Review an Internal Gear Honing,” *International Journal of Engineering Research & Technology (IJERT)* Vol. 2 Issue 5
- [6] N Amini, H Westberg, F Klocke and T K öllner 1999 “An Experimental Study on the Effect of Power Honing on Gear Surface Topography,” *Gear Technology, Vol. 16* pp 11–18
- [7] V T Tran, R H Hsu and C B Tsay 2014 “Study on the Anti-Twist Helical Gear Tooth Flank with Longitudinal Tooth Crowning,” *Journal of Mechanical Design* Vol. 136 pp 061007 (1–10)
- [8] V T Tran, R H Hsu and C B Tsay 2015 “A Crowned Helical Gear with Twist-free Tooth Flanks Generated by A CNC Honing Machine,” *International Journal of Mechanical and Production Engineering* Vol. 3 Issue 1
- [9] Y R Wu and V T Tran 2015 “Lead Crowning and Anti-twist for Tooth Flank of a Heat Treated Helical Gear on Internal CNC Honing Machine,” *Applied Mechanics and Materials* Vol. 799–800 pp 554–59
- [10] Y R Wu and V T Tran 2016 “Transmission and Load Analysis for A Crowned Helical Gear Pair with Twist-free Tooth Flanks Generated by An External Gear Honing Machine,” *Mechanism and Machine Theory* Vol. 98 pp 36–47
- [11] F L Litvin 1994 *Gear Geometry and Applied Theory*, PTR Prentice Hall, Englewood Cliffs, NJ pp 412–68